Weighted-permutation entropy: A complexity measure for time series incorporating amplitude information

Bilal Fadlallah,[1,*] Badong Chen,[2,†] Andreas Keil,[3] and José Príncipe[1,*]

[1]*Computational NeuroEngineering Laboratory, Department of Electrical and Computer Engineering, University of Florida, Gainesville, Florida 32611, USA*

[2]*Institute of Artificial Intelligence and Robotics, Xi'an Jiaotong University, Xi'an 710049, China*

[3]*NIMH Center for the Study of Emotion and Attention, Department of Psychology, University of Florida, Gainesville, Florida 32611, USA*

(Received 6 March 2012; revised manuscript received 5 December 2012; published 20 February 2013)

Permutation entropy (PE) has been recently suggested as a novel measure to characterize the complexity of nonlinear time series. In this paper, we propose a simple method to address some of PE's limitations, mainly its inability to differentiate between distinct patterns of a certain motif and the sensitivity of patterns close to the noise floor. The method relies on the fact that patterns may be too disparate in amplitudes and variances and proceeds by assigning weights for each extracted vector when computing the relative frequencies associated with every motif. Simulations were conducted over synthetic and real data for a weighting scheme inspired by the variance of each pattern. Results show better robustness and stability in the presence of higher levels of noise, in addition to a distinctive ability to extract complexity information from data with spiky features or having abrupt changes in magnitude.

DOI: 10.1103/PhysRevE.87.022911 PACS number(s): 05.45.Tp, 05.40.−a, 02.50.−r

I. INTRODUCTION

There is little consensus on the definition of a signal's complexity. Among the different approaches, entropy-based ones are inspired by either nonlinear dynamics [1] or symbolic dynamics [2,3]. Permutation entropy (PE) has been recently suggested as a complexity measure based on comparing neighboring values of each point and mapping them to ordinal patterns [2]. Using ordinal descriptors is helpful in the sense that it adds immunity to large artifacts occurring with low frequencies. PE is applicable for regular, chaotic, noisy, or real-world time series and has been employed in the context of neural [4], electroencephalographic (EEG) [5–8], electrocardiographic (ECG) [9,10], and stock market time series [11]. In this paper, we suggest a modification that alters the way PE handles the patterns extracted from a given signal by incorporating amplitude information. For many time series of interest, the new scheme better tracks abrupt changes in the signal and assigns less complexity to segments that exhibit regularity or are subject to noise effects. Examples include any time series containing amplitude-coded information. For such signals, the suggested method has the advantage of providing immunity to degradation by noise and (linear) distortion.

The paper is organized as follows. In Secs. II and III, we briefly introduce permutation entropy and formulate weighted-permutation entropy. Simulations details are presented in Sec. IV, respectively, on synthetic, single channel and dense-array EEG, and epileptic data. Section V offers discussion and concluding remarks.

II. PERMUTATION ENTROPY

Consider the time series $\{x_t\}_{t=1}^{T}$ and its time-delay embedding representation $X_j^{m,\tau} = \{x_j, x_{j+\tau}, \ldots, x_{j+(m-1)\tau}\}$ for $j = 1,2,\ldots,T-(m-1)\tau$, where m and τ denote, respectively, the embedding dimension and time delay. To compute PE, each of the $N = T-(m-1)\tau$ subvectors is assigned a single motif out of $m!$ possible ones (representing all unique orderings of m different real numbers). PE is then defined as the Shannon entropy of the $m!$ distinct symbols $\{\pi_i^{m,\tau}\}_{i=1}^{m!}$, denoted as Π:

$$H(m,\tau) = -\sum_{i:\pi_i^{m,\tau}\in\Pi} p\left(\pi_i^{m,\tau}\right)\ln p\left(\pi_i^{m,\tau}\right). \tag{1}$$

$p(\pi_i^{m,\tau})$ is defined as

$$p\left(\pi_i^{m,\tau}\right) = \frac{\left\|\left\{j : j \leqslant N, \text{type}\left(X_j^{m,\tau}\right) = \pi_i^{m,\tau}\right\}\right\|}{N}, \tag{2}$$

where type(.) denotes the map from pattern space to symbol space and $\|.\|$ denotes the cardinality of a set. An alternative way of writing $p(\pi_i^{m,\tau})$ is

$$p(\pi_i^{m,\tau}) = \frac{\sum_{j\leqslant N}\mathbf{1}_{u:\text{type}(u)=\pi_i}\left(X_j^{m,\tau}\right)}{\sum_{j\leqslant N}\mathbf{1}_{u:\text{type}(u)\in\Pi}\left(X_j^{m,\tau}\right)}, \tag{3}$$

where $\mathbf{1}_A(u)$ denotes the indicator function of set A defined as $\mathbf{1}_A(u) = 1$ if $u \in A$ and $\mathbf{1}_A(u) = 0$ if $u \notin A$. PE assumes values between in the range $[0, \ln m!]$ and is invariant under nonlinear monotonic transformations.

The main shortcoming in the above definition of PE resides in the fact that no information besides the order structure is retained when extracting the ordinal patterns for each time series. This may be inconvenient for the following reasons: (i) most time series have information in the amplitude that might be lost when solely extracting the ordinal structure; (ii) ordinal patterns where the amplitude differences between the time series points are greater than others should not contribute similarly to the final PE value; and (iii) ordinal patterns resulting from small fluctuations in the time series can be due to the effect of noise and should not be weighted

*{bhf, principe}@cnel.ufl.edu
†chenbd@mail.xjtu.edu.cn

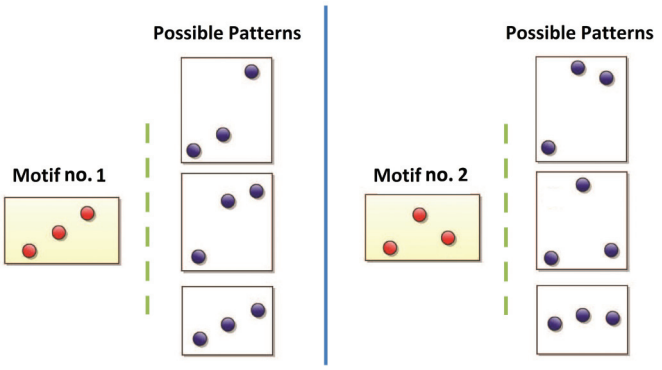

FIG. 1. (Color online) Two examples of possible m-dimensional vectors corresponding to the same motif. The value of m used is 3.

uniformly toward the final value of PE. Figure 1 shows how the same ordinal pattern can originate from different m-dimensional vectors.

III. WEIGHTED-PERMUTATION ENTROPY

To counterweight these facts, we propose a modification of the current PE procedure to incorporate significant information from the time series when retrieving the ordinal patterns. The main motivation lies in saving useful amplitude information carried by the signal.

We refer to this procedure as weighted-permutation entropy (WPE) and summarize it in the following steps. First, the weighted relative frequencies for each motif are calculated as follows:

$$p_w\left(\pi_i^{m,\tau}\right) = \frac{\sum_{j\leqslant N} \mathbf{1}_{u:\text{type}(u)=\pi_i}\left(X_j^{m,\tau}\right) w_j}{\sum_{j\leqslant N} \mathbf{1}_{u:\text{type}(u)\in\Pi}\left(X_j^{m,\tau}\right) w_j} \tag{4}$$

WPE is then computed as

$$H_w(m,\tau) = -\sum_{i:\pi_i^{m,\tau}\in\Pi} p_w\left(\pi_i^{m,\tau}\right) \ln p_w\left(\pi_i^{m,\tau}\right). \tag{5}$$

Note that when $w_j = \beta \;\; \forall\; j \leqslant N$ and $\beta > 0$, WPE reduces to PE. It is also interesting to highlight the difference between the definition of weighted entropy in this context and previous ones suggested in the literature. Weighted entropy, defined as $H_{we} = -\sum_k w_k p_k \ln p_k$, has been suggested as a variant to entropy that uses a probabilistic experiment whose elementary events are characterized by weights w_k [12]. WPE, on the other hand, extends the concept of PE while keeping the same Shannon's entropy expression reflected by Eq. (5), hence weights are added prior to computing the $p(\pi_i^{m,\tau})$. The choice of weight values w_i is equivalent to selecting a specific (or combination of) feature(s) from each vector $X_j^{m,\tau}$. Such features may differ according to the context used. Note that the relation $\sum_i p_w(\pi_i^{m,\tau}) = 1$ still holds. In this paper, we use the variance or energy of each neighbors vector $X_j^{m,\tau}$ to compute the weights. Let $\bar{X}_j^{m,\tau}$ denote the arithmetic mean of $X_j^{m,\tau}$, or

$$\bar{X}_j^{m,\tau} = \frac{1}{m}\sum_{k=1}^{m} x_{j+(k+1)\tau}. \tag{6}$$

We can hence express each weight value as

$$w_j = \frac{1}{m}\sum_{k=1}^{m}\left[x_{j+(k-1)\tau} - \bar{X}_j^{m,\tau}\right]^2. \tag{7}$$

The motivation behind this setting is to specifically counteract the limitations discussed in the previous section, i.e., weight differently neighboring vectors having the same ordinal patterns but different amplitude variations. In this way, WPE can be also used to detect abrupt changes in noisy or multicomponent signals. The modified $p(\pi_i^{m,\tau})$ can be then thought of as the proportion of variance accounted for by each motif. The above definition of WPE retains most of PE's properties and is invariant under affine linear transformations. WPE, however, presents a specificity, given it incorporates amplitude information and demonstrates more robustness to noise.

IV. SIMULATIONS

An adequate testing scheme would include spiky data because it poses a challenge to a simple motif count approach and exhibits sudden changes. Simulations were performed on both synthetic data and EEG data.

A. Synthetic data

As a first motivation, we suggest analyzing the behavior of PE and WPE in the presence of an impulsive and noisy signal. Figure 2(a) shows 1000 samples of a signal consisting of an impulse and additive white Gaussian noise (AWGN)

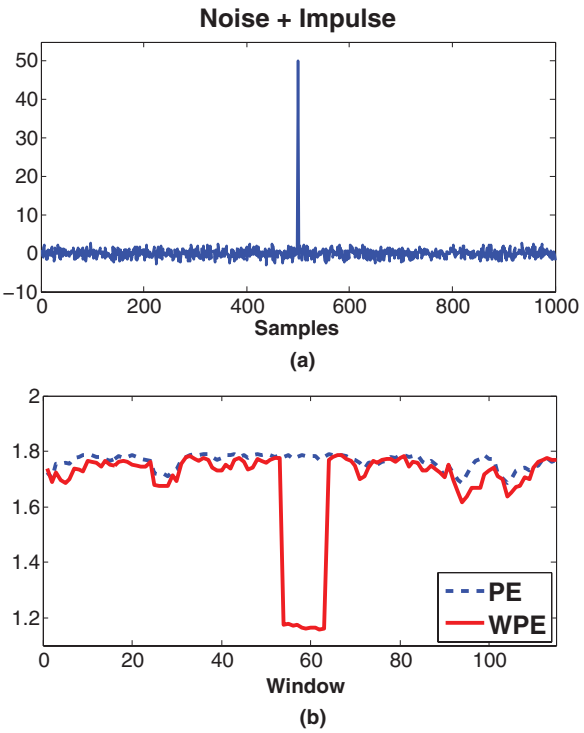

FIG. 2. (Color online) PE versus WPE in the case of an impulse. (a) Impulse with additive white Gaussian noise with zero mean and unit variance. (b) Computed PE and WPE values with windows of 80 samples slid by 10 samples. A remarkable drop in the value of WPE is noticed in the impulse region for which PE values do not show any marked change.

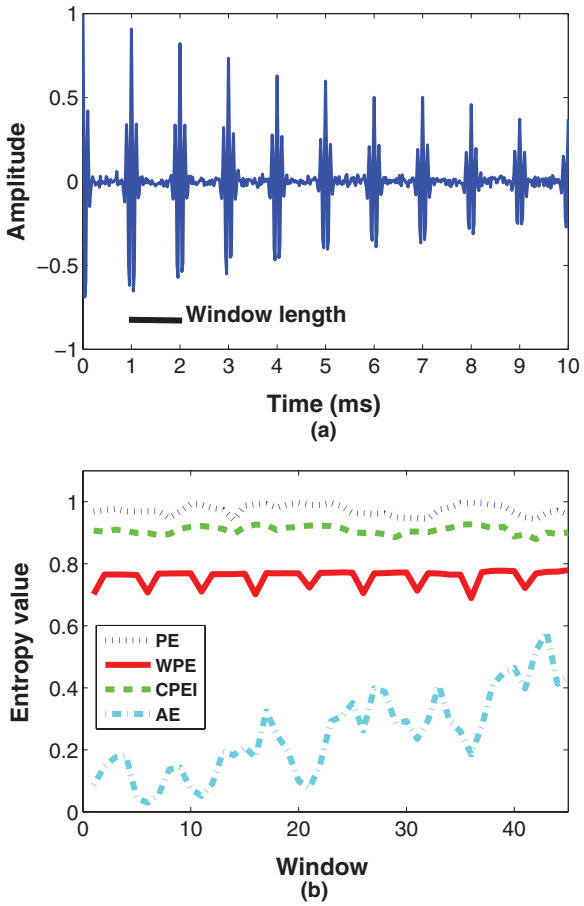

FIG. 3. (Color online) Different entropy measures (PE, WPE, CPEI, and AE) applied on a Gaussian-modulated sinusoidal train with a frequency of 10 kHz, a pulse repetition frequency of 1 kHz and an amplitude attenuation rate of 0.9. Initial signal was corrupted by additive white Gaussian noise (AWGN) having mean $\mu = 0$ and variance $\sigma^2 = 0.2$. The sampling rate was 50 kHz and computations used a 50-sample sliding window with increments of 10 samples. The recorded SNR was of 4.8 dB.

with zero mean and unit variance. Windows of 80 samples slid by 10 samples were used and results were averaged over 10 simulations. A remarkable drop in the value of WPE is noticed in the impulse region. No marked change can be observed in the case of PE for the same region.

As the next step, we try a train of Gaussian-modulated sinusoidal pulses with decaying amplitudes. The value of τ was set to 1. Sliding windows of 50 samples with increments of 10 samples were used and m was set to 3. Again, the signal was corrupted by AWGN and simulations were run across different variance levels. Figure 3 shows the variations of the signal's entropy for four different methods. The performance of PE and WPE is compared to two other methods from the literature, namely approximate entropy or ApEn [1,13] and the composite PE index or CPEI [14]. In the following, we give a brief description of each.

Approximate entropy (ApEn or AE) is a measure that quantifies the regularity or predictability of a time series. It is defined with respect to a free parameter r as follows:

$$H_a = \Phi^m(r) - \Phi^{m+1}(r), \tag{8}$$

where $\Phi^m(r)$ is defined as

$$\Phi^m(r) = \frac{1}{N-(m-1)\tau} \sum_{i=1}^{N-(m-1)\tau} \ln C_i^m(r) \tag{9}$$

and $C_i^m(r)$ is defined using the Heavyside function $\Theta(u)$ (1 for $u > 0$, 0 otherwise) and a distance measure dist:

$$C_i^m(r) = \frac{\sum_{j=1}^{N-(m-1)\tau} \Theta\left[r - \mathrm{dist}\left(X_i^{m,\tau}, X_j^{m,\tau}\right)\right]}{N-(m-1)\tau}. \tag{10}$$

Here the value of r is set to be 0.2 times the data standard deviation as per the thorough discussion in Ref. [13]. The distance measure we use is the same suggested in Ref. [1] and can be formulated as

$$\mathrm{dist}\left(X_i^{m,\tau}, X_j^{m,\tau}\right) = \max_{k=1,\ldots,m} \mid x_{i+(k-1)\tau} - x_{j+(k-1)\tau} \mid$$

The composite PE index (CPEI) is an alteration of permutation entropy that differentiates between the types of patterns. It is calculated as the sum of two permutation entropies corresponding to motifs having different *delays*, where the latter (denoted as τ in this paper) is determined by whether the motif is monotonically decreasing or increasing. CPEI, which we denote by H_i in this paper, responds rapidly to changes in EEG patterns and can be defined as follows [14]:

$$H_i = \frac{1}{\ln(m!+1)} \frac{H(m,1) + H(m,2)}{2}. \tag{11}$$

The normalization denominator in Eq. (11) consists of the original number of motifs in addition to a newly introduced motif to account for ties (ties describe cases where negligible differences in amplitude occur within a motif). As a side note, the averaging step performed in that equation is highly approximative because of the lack of independency between motifs at different delays.

It is noticeable that WPE consistently drops for portions of the signal showing pulses. This is desired because of the lesser complexity of these regions and expected because of their immunity to noise. Here we assume that the information contained in the examined signals is amplitude-dependent. Such results meet our expectations since WPE is clearly able to differentiate between bursty and stagnant regions of the pulse train. In other words, using the variance contributes to weakening the noise effects and assigning more weight to the regular spiky patterns corresponding to a higher amount of information, which results in easier predictability and less complexity. It is important to note two things: (1) the contribution of patterns with higher variance toward the value of WPE dominates those of patterns with lesser variance, which highlights the powerfulness of the method in detecting abrupt changes in the input signal and (2) the fact that WPE is computed within a specific time window explains why WPE values corresponding to impulsive segments of the signal do not decrease in spite of the decreasing amplitudes of the spikes [the normalization effect in Eq. (4) takes place within each window]. We also plot in Fig. 4 the values of PE and WPE for different levels of signal-to-noise ratio (SNR). As anticipated, both entropy measures decrease with the increase of the SNR since the effect of noise contributing to more complexity

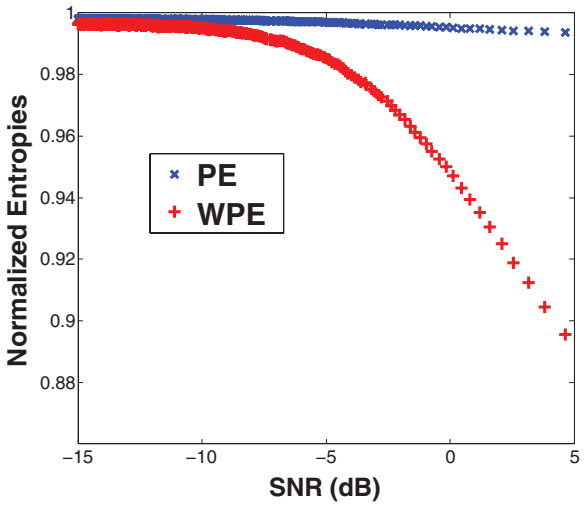

FIG. 4. (Color online) Normalized PE and WPE values for different SNR levels. The signal used is the same as that described in the legend of Fig. 3.

becomes less significant. WPE decreases at a higher pace than PE, which reflects a better robustness to noise. As a final note on this section, we point out that traditional methods like zero-crossing spike detection techniques might be useful for the purpose of this simulation; however, the sought goal was to demonstrate, using synthetic data, the ability of WPE to discriminate between regimes of data.

B. Single-channel EEG data analysis

In Fig. 5, the same comparisons are performed for a sample EEG recording processed as in Ref. [15]. Highpass filtering was further applied on the signal because we are interested in removing very low frequency components. It can be seen that WPE locates the regions where abrupt changes occur in the initial signal more accurately than the other methods, which is inline with our original expectations. The same is reflected in Fig. 6, which shows a processed EEG portion corresponding to another channel. Our simulations show that increasing m beyond 4 affects the running time without significantly changing the obtained entropies. This is inline with the findings in Ref. [16], where the parameter selection problem has been addressed, and Ref. [14]. For situations where the effect of m is more pronounced, the running time issue can be addressed by speeding up the sliding of the window as this entails a higher number of affected patterns at each instance.

C. Multichannel EEG data analysis

Setting. We propose to tackle the problem suggested in Ref. [15] from the perspective of the method presented above. The experimental setting exploits the steady-state visual evoked potential (ssVEP) paradigm by flashing a visual stimulus at a rate of 17.5 Hz to a participant. Two types of stimuli were presented to the subject, one representing an image of a neutral human face and the second a Gabor patch (Fig. 7). Each stimulus was presented for 4.2 sec (plus 0.4 sec prestimulus baseline). A surface Laplacian method

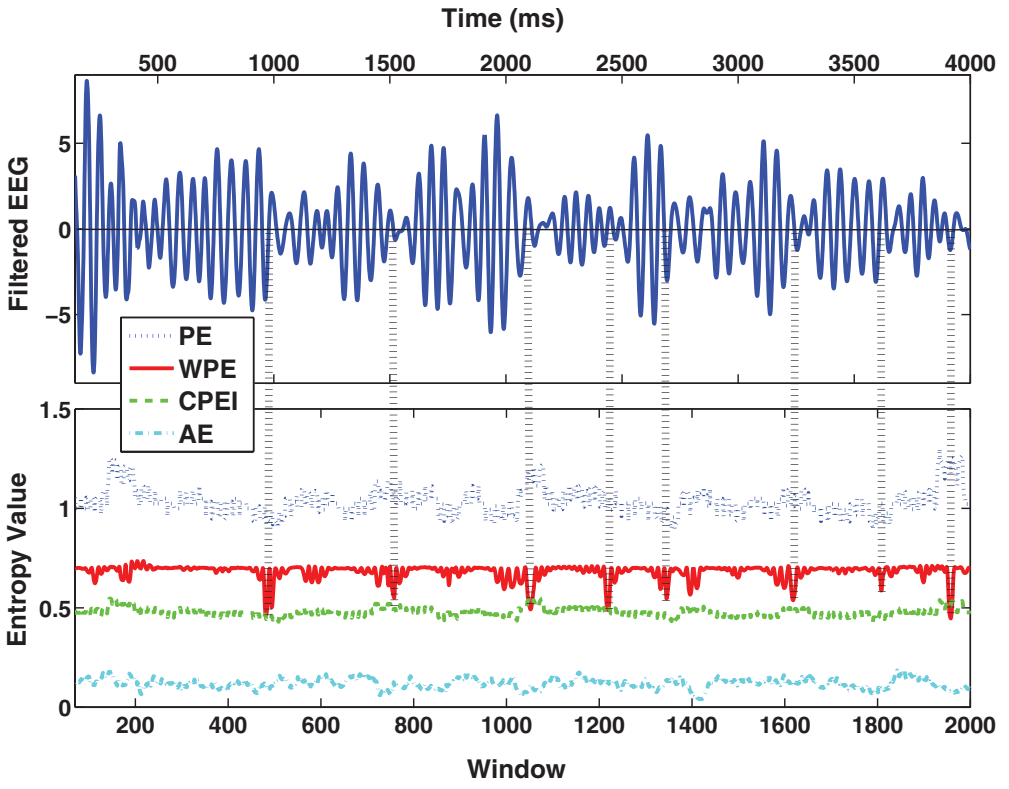

FIG. 5. (Color online) Simulations performed on filtered EEG data sampled at 1000 Hz and processed as in Ref. [15]. WPE outperforms other entropy measures in location regiments exhibiting abrupt changes in the signal. The window length used for this plot was 114 with an overlap of two samples.

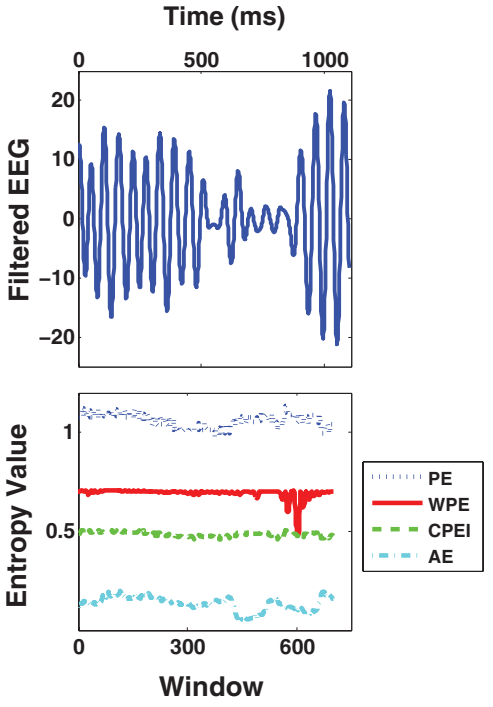

FIG. 6. (Color online) Same procedure applied on a processed EEG portion corresponding to another channel. WPE mirrors best the sharp change in the signal noticeable before $t = 850$ ms. The window size used was 200 with an overlap of two samples at each iteration.

was applied on the raw EEG data and the experiment's objective was to identify the active regions involved in the cognitive processing of each stimulus and study the corresponding connectivity patterns between all channel locations. In Ref. [18], two traditional coupling methods (Pearson's correlation and mutual information) and one novel approach termed "generalized measure of association" (or GMA) were used to calculate bivariate interactions with respect to a single parieto-occipital channel chosen as reference (channel PO_z in a standard 10–20 referential configuration). Dependence values were computed per time windows of 114 samples.

The rationale for choosing this specific time window can be summarized as follows: the selected window size

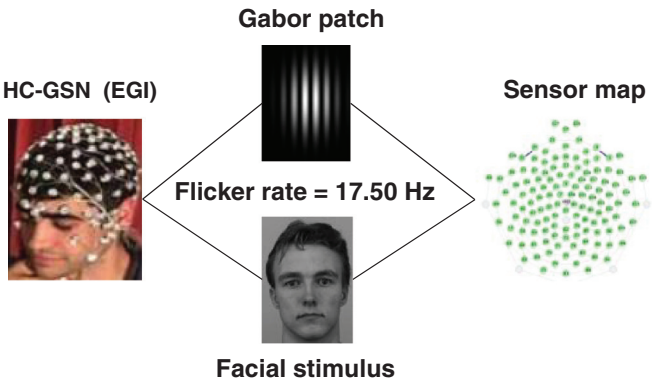

FIG. 7. (Color online) Experimental setting using a HydroCell Geodesics Sensor Networks system from Electrical Geodesics, Inc. [17].

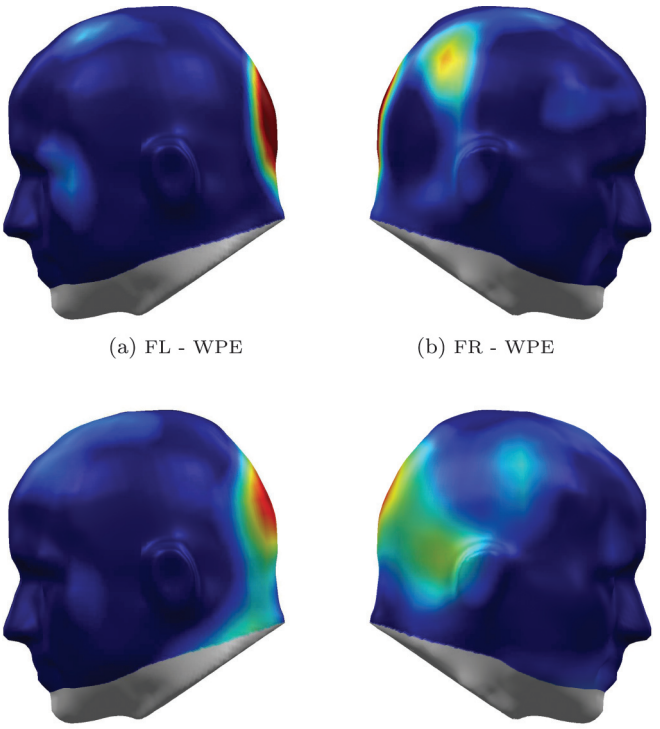

(a) FL - WPE (b) FR - WPE

(c) FL - PE (d) FR - PE

FIG. 8. (Color online) Using Spearman's correlation to weight graph connections for channel 72. First two subplots (a and b) show interpolated correlation measures over right and left (R and L) head surface for the face condition (F) when using WPE, and subsequent subplots (c and d) exhibit the same when using PE. A statistical assessment of the discriminatory performance between the two conditions can be seen in Fig. 9 and Table I (results for Gabor condition were not reported due to lack of space).

should (1) allow tracking the signal behavior with high time resolution, i.e., using a reduced number of samples, (2) include enough samples that allow the estimation of permutation entropy quantities, and (3) relate to the observed physiological properties of the cognitive system being studied. Setting the window size to 114 verifies the three conditions (since 114 samples correspond to two periods of the ssVEP signal and roughly matches the propagation time between brain cortices). Using this setting, higher coupling was observed for the face condition between occipital sites and the temporal-parietal-occipital sites neighboring $P4$. The methodology suggested in this paper will be applied on the same experimental data to infer functional relationships across different electrode sites.

Procedure. A precursor for a useful usage of PE (WPE) within the above context is to assign a "complexity" curve for each recorded signal, corresponding to an array of PE (WPE) values computed over a given time window (114 ms in this case). We can then compute the dependence between the different channels by simply applying correlation on these curves. Intuitively, this implies using a linear measure of dependence to measure how close the complexity of two time series are. In our simulations, we select Spearman's ρ as a measure of statistical dependence between the different PE (WPE) curves. In Fig. 8, the obtained correlation values are mapped onto the corresponding locations on the human scalp.

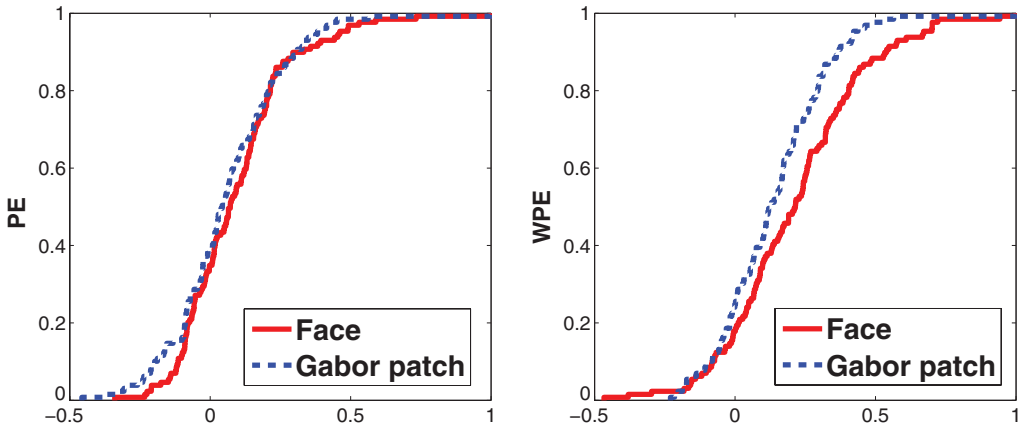

FIG. 9. (Color online) Empirical cumulative distribution functions (CDFs) per condition for PE and WPE.

In the case of WPE [Figs. 8(a) and 8(b)], more activity can be spotted in locations that seem to point toward sources in the occipito-parieto-temporal area of the right brain hemisphere. This outcome aligns with the results obtained in Ref. [18], which, as previously mentioned, indicate higher activity in that specific region. On the other hand, PE tends to show activity localized in right posterior areas.

Statistical analysis. We use the two-sample Kolmogorov-Smirnov (KS) test applied on the obtained distributions with the null hypothesis being that the two samples are drawn from the same distribution. The KS test tries to estimate the distance between the empirical distribution functions of the two samples. Assuming $\boldsymbol{\gamma}_1(x)$ and $\boldsymbol{\gamma}_2(x)$ to be the sample vectors, it can be calculated as $K_{\boldsymbol{\gamma}_1,\boldsymbol{\gamma}_2} = \max_x |F_{\boldsymbol{\gamma}_2}(x) - F_{\boldsymbol{\gamma}_1}(x)|$, where $F_{\boldsymbol{\gamma}_1}(x)$ and $F_{\boldsymbol{\gamma}_2}(x)$ denote the empirical cumulative distribution functions for the n iid observations; alternatively, $F_{\{X_1,\ldots,X_n\}}(x) = \frac{1}{n}\sum_{i=1}^{n} I_{X_i \leqslant x}$, where I_k denotes the indicator function. The null hypothesis is rejected at the α level if $\sqrt{(n_1 n_2)/(n_1+n_2)}S_{\boldsymbol{\gamma}_1,\boldsymbol{\gamma}_2} > K_\alpha$, where n_1 and n_2 denote the number of samples from each observation vector and K refers to the Kolmogorov distribution [19]. In our case, $n_1 = n_2 = 45$ and $\alpha = 0.05$.

Discussion. Figure 9 and Table I show that, unlike PE, WPE is able to discriminate the two conditions with a statistically significant KS test. A possible explanation is the inconsistency in PE's tracking of steep changes in the processed signals, which creates ad hoc dependencies when computing the pairwise correlations and results in the indiscernibility of the two conditions. This problem is avoided when using WPE since the latter follows faithfully the change trends in the signal as illustrated in Fig. 3.

D. Epilepsy detection

Setting. Next we propose to apply WPE for epilepsy detection. We use the same data as Quiroga *et al*. [20,21], in which tonic-clonic seizures of a subject were recorded with a scalp right central electrode (located near $C4$ in a standard 10–20 montage). The recording consisted of 3 min, including around 1 min of preseizure time and 20 sec of postseizure

TABLE I. Two-sample Kolmogorov-Smirnov test results

KS test	PE	WPE
Null hypothesis rejection	False	True
p value	0.508	0.009
Test statistic	0.101	0.202

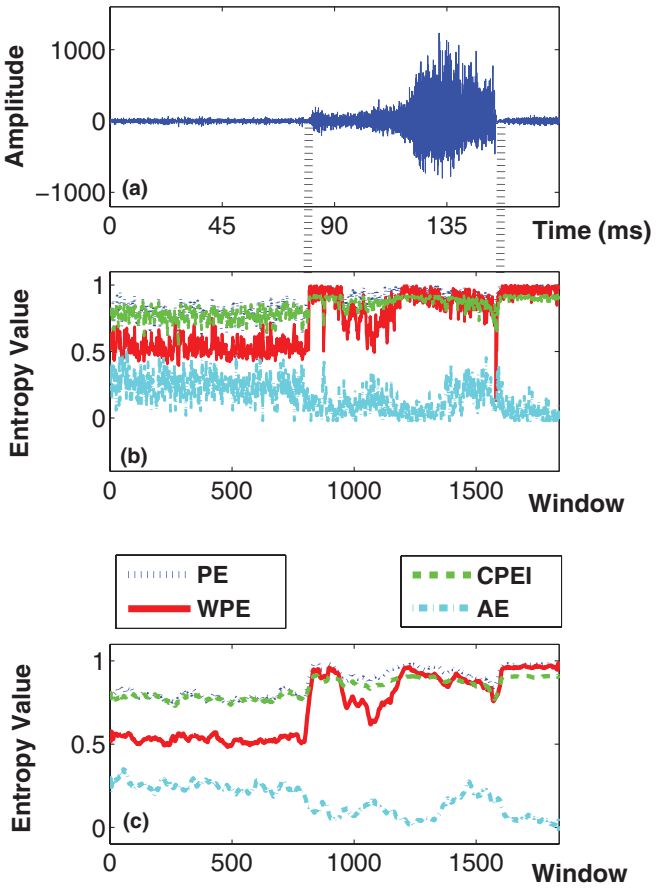

FIG. 10. (Color online) Different entropy-based measures applied on epileptic EEG. (a) EEG recording of an epileptic subject. The recording, sampled at 102.4 Hz contains approximately 1 min of preseizure activity and 20 sec of postseizure activity. (b) Different measures of entropy computed using a sliding window of 50 samples with 5 samples overlap. (c) Smoothed entropy measures curves obtained by applying a moving average filter of length 35 samples.

TABLE II. Ratio of average measured entropy between epileptic and nonepileptic segments

Measure	Ratio[a]
Permutation Entropy (PE)	1.27
Weighted-Permutation Entropy (WPE)	1.85
Composite Permutation Entropy Index (CPEI)	1.30
Approximate Entropy (AE)	0.57

[a]Entropy values corresponding to the epileptic EEG segment were averaged and divided by the average corresponding to the nonepileptic part.

activity. A sampling rate of 102.4 Hz was used to collect the signal.

Discussion. We computed different measures of entropy on windows of 50 samples of data slid by 5 samples [Fig. 10(b)]. The obtained curves are further smoothed in Fig. 10(c) using a moving average filter of length 35 samples. The commencement of epileptic activity in the recorded signal induces noticeable changes for all entropy measures, in particular for WPE that exhibits a significant jump in value. This is further quantified by computing the ratio of average measured entropies of epileptic and nonepileptic segments (Table II), which shows a more pronounced difference between both portions for WPE. The latter achieves almost twice better discriminability between the two portions of the signal, i.e., 42% better than the next closest measure (CPEI).

V. CONCLUSION

This paper proposes a different definition of permutation entropy that retains amplitude information of nonlinear time series. A method to weight the motif counts by statistics derived from the signal patterns has been proposed. The new method is different from PE, however, in the sense that it suits better signals having considerable amplitude information. For the range of signals that do not verify this property, PE might be a better choice. Simulations were carried on spiky synthetic data and human EEG recordings that underwent narrow-band filtering, taking into account the variance of the mentioned patterns. The measure showed consistency when applied on various regions of both signals by differentiating distinct regimes and assigning similar complexities for analogous portions. Moreover, WPE decreases for higher SNRs, which corroborates the fact that noise has higher complexity. The suggested method was also applied on processed EEG data to differentiate two cognitive states as suggested in Ref. [18], with the help of the Kolmogorov-Smirnov statistical tool, and epileptic data to detect seizure onset. The power of permutation entropy as a simple and computationally fast measure for time series complexity has been hence confirmed on both synthetic and real data. Future work includes analyzing more thoroughly the effect of the free parameters (m, noise model,...), exploring other weighting schemes, and comparing to other nonlinear regularity estimators based on equiquantal or equiprobable binning.

ACKNOWLEDGMENTS

This work was supported by the U.S. National Science Foundation under Grant No. IIS-0964197 and the Lebanese Center for Scientific Research (CNRS). The authors thank Austin Brockmeier for useful discussion and the anonymous reviewers for their constructive suggestions.

[1] S. Pincus, Proc. Natl. Acad. Sci. USA **88**, 2297 (1991).
[2] C. Bandt and B. Pompe, Phys. Rev. Lett. **88**, 174102 (2002).
[3] J. Kurths, U. Schwarz, A. Witt, R. Th. Krampe, and M. Abel, AIP Conf. Proc. **375**, 33 (1996).
[4] Z. Li, G. Ouyang, D. Li, and X. Li, Phys. Rev. E **84**, 021929 (2011).
[5] X. Li, S. Cui, and L. Voss, Anesthesiology **109**, 448 (2008).
[6] X. Li, G. Ouyang, and D. Richards, Epilepsy Res. **77**, 70 (2007).
[7] A. Bruzzo, B. Gesierich, M. Santi, C. Tassinari, N. Birbaumer, and G. Rubboli, Neurol. Sci. **29**, 3 (2008).
[8] Y. Cao, W. W. Tung, J. B. Gao, V. A. Protopopescu, and L. M. Hively, Phys. Rev. E **70**, 046217 (2004).
[9] B. Graff, G. Graff, and A. Kaczkowska, Acta Phys. Pol. B **5**, 153 (2012).
[10] D. Zhang, G. Tan, and J. Hao, Int. J. Hybrid Info. Technol. **1**, 1 (2008).
[11] L. Zunino, M. Zanin, B. Tabak, D. Perez, and O. Rosso, Physica A **388**, 2854 (2009).
[12] S. Guiasu, Rep. Math. Phys. **2**, 165 (1971).
[13] K. Chon, C. Scully, and L. Sheng, IEEE Eng. Med. Biol. Mag. **28**, 18 (2009).
[14] E. Olofsen, J. Sleigh, and A. Dahan, Br. J. Anaesth. **101**, 810 (2008).
[15] B. H. Fadlallah, S. Seth, A. Keil, and J. Principe, *33rd Annual International Conference of the IEEE EMBS, Boston, MA* (IEEE, New York, 2011), pp. 1407–1410.
[16] M. Staniekand and K. Lehnertz, Int. J. Bifurcat. Chaos **17**, 3729 (2007).
[17] Electric Geodesics Inc. (2007), http://www.egi.com
[18] B. Fadlallah, S. Seth, A. Keil, and J. Principe, IEEE Trans. Biomed. Eng. **59**, 2773 (2012).
[19] G. Marsaglia, W. Tsang, and J. Wang, J. Stat. Soft. **8**, 1 (2003).
[20] R. Quian Quiroga, S. Blanco, O. A. Rosso, H. Garcia, and A. Rabinowicz, Electroenceph. Clin. Neurophysiol. **103**, 434 (1997).
[21] R. Quian Quiroga, H. Garcia and A. Rabinowicz, Electromyogr. Clin. Neurophysiol. **42**, 323 (2002).